DETERMINATION OF CLOUD PROPERTIES FROM THERMAL RADIATION MEASUREMENTS AT 10 to 18 μm

A.K. Gorodetskii

Institute of Space Research, USSR Academy of Sciences
Received June 13, 1988

The emissivity of different types of clouds was derived from airborne measurements at 10 to 18 μm region. The measurements of radiation from clouds and atmospheric counterradiation were accompanied by measurements of meteorological parameters. The values of the cloud emissivity thus obtained were used to develop remote techniques for measuring the properties of clouds on the basis of spectral and angular distributions of the emitted intensity. Comprehensive simultaneous measurements in the visible and IR allowed the cloud-top temperature and height to be estimated, and in combination with observations in the microwave region also provided for determination of the cloud phase state.

The middle IR is widely used for determining such parameters as cloud temperature T_c, amount of cloud cover n_c, and cloud-top height h_c[1,2]. To convert from the radiation temperature $T_r(\nu)$ to height, single-channel and multichannel approaches have been developed[2–4]. Information on the cloud phase state is obtained from measurements of the solar radiation reflected from clouds in the absorption bands of liquid water and ice[3,5] as well as from microwave measurements[6]. The majority of the techniques are based on the simplifying assumption that clouds have a monolayered and optically thick structure whose emissivity ε_ν is equal to unity. The development of techniques accounting for the variety of cloud forms requires experimental data, with the most reliable measurements being airborne observations. This paper presents the results of airborne[7] and spaceborne[8] (Kosmos-1151) measurements of the radiative properties of clouds. Measurements of radiation emitted from cloud tops were carried out from an IL-14 aircraft using a radiometer in the 10.5–12 μm range. The radiation temperature measurements were supplemented with meteorological data on pressure, temperature $T_a(p)$ and relative humidity $a(p)$. The equipment included also involved a nephelometer used to determine the cloud backscattering coefficient $\sigma(0.53)$ at $\lambda = 0.53$ μm[9].

The instrumentation was flown over the cloud tops and below the cloud deck, which enabled us to estimate the cloud emissivity for both upward- and downward-directed radiation. To allow for atmospheric counterradiation we measured the radiation incident upon the cloud tops layer $I_\nu^\downarrow(m)$, $m = \sec\theta$ (where θ is the zenith angle) and the upward-directed radiation from below the cloud deck $I_\nu^\uparrow(m)$ to derive the cloud-top ε_ν.

$$\varepsilon_\nu = (I_\nu - I_\nu^\downarrow)/\{B_\nu[T_a(h_c)] - I_\nu^\downarrow\} \quad (1)$$

The errors in ε_ν originate from a partial transparency of clouds and a contribution from the overcloud inversion layers. In the case of semitransparent clouds, the ε_ν-measurements will exhibit large uncertainties due to terrestrial radiation. Therefore we selected for our studies only optically thick clouds for which $T_r(\nu) < T_a(h_c)$, where $T_r(\nu)$ is the cloud radiation temperature, and $T_a(h_c)$ is the air temperature at the cloud top level. The results obtained from the measurements are summarized Table 1, where maximum (1) and minimum (2) values of ε_ν sire given for different cloud types. Realizations 1–5 refer to the cloud-top measurements and realization 6 represents cloud-base observations. It is seen from Table 1 that for the different types of clouds, $0.92 \le \varepsilon_\nu \le 1$. The variations of the cloud emissivity reflect to acertain degree the variability of macro- and microphysical properties of clouds. The latter becomes apparent from different mean values, statistical moments, and the distribution density of the backscattering coefficient $\sigma(0.53)$ (see Fig. 1, Table 2), and that of the optical depth $\tau(0.74)$ extracted from the measured reflected solar radiation using Rozenberg's asymptotic formulas[10,11].

The difference of ε_ν from unity is manifested in the angular dependence of the cloud radiation intensity for upward- and downward-directed emission.

Figure 2 presents $I(m)/I(m = 1)$ calculated for the spectral range 11.1 ± 0.37 μm using Kosmos-1151 satellite images of high clouds with a radiation temperature of 220 – 240 K[8]. Also shown in Figure 2 is the angular distribution of $I_\nu(m)/B_\nu(T_c)$ at the cloud base[7] estimated from airborne measurements. In the case of downward radiation, $\varepsilon_\nu(m)$ is seen to have a nonmonotonic pattern resulting from the vertical temperature profile in the cloud-base layer, an Increase in the optical depth in the lowest, warmest part of the cloud with e, and enhanced cloud reflectivity.

Table 1. Emissivlty of clouds ε_ν in the 10.5 to 12 μm range, h_1 and T_1 are cloud botton height and temperature, respectively.

	Cloud Form , Type	Cloudtop height, h_c thickness Δh_c km		Cloudtop Temperature T_c °C, Lapse Rate $\frac{\Delta T}{\Delta h}$ deg/km		Emissivity ε_ν	
		(1)	(2)	(1)	(2)	(1)	(2)
1.	Sc cuf op partially inversion	1.7 0.32	1.81 0.26	-1.4 4.2	-6.5 5.0	0.99	0.94
2,	Ac noninversion semitranspa-rent	4.9 0.46	3.3 1.3	-16.5 8.1	-7.2 4.7	1.0	0.95
3.	Ac subinversion	2.8 0.17	3.7 0.35	-9.5 6.0	-2.3 6.7	0.99	0.935
4.	Cu partially inversion	2.9 1.4	1.4 *	-13.0 4.8	-12.0	0.92	0.91
5.	Cu subinversion	2.08 1.2	2.0 1.05	-6.1 6.0	-6.0 5.9	0.94	0.93
6.	Sc	0.5 0.5	h_1	22.3 8.0	T_1	0.96	0.93

Table 2. Backscattering coefficients σ(0.53) for different cloud types

	Cloud Type	Mean value $\bar{\sigma}$ km^{-1}	r.m.s. deviation $\Delta\bar{\sigma}$ km	Data from reference 14
1.	*Ns-As* closely adjacent to frontal zone	24.3	13.5	28.6
2.	*Ns-As* 200 km away from precipi-tation zone	6.3	4.1	-
3.	*St*	37.0	16.4	42.6
4.	*Sc*	18.1	12.3	47.5
5.	*As*	7.0	4.1	25.5

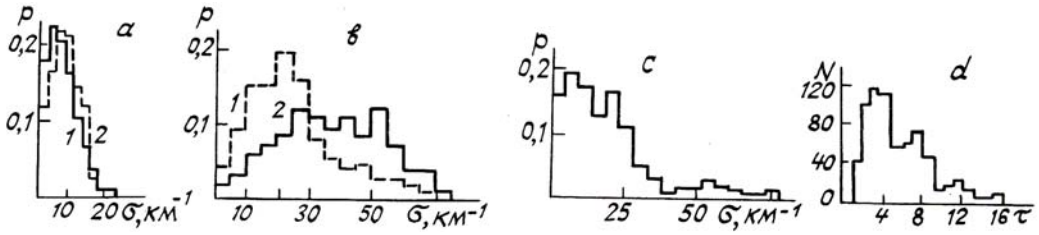

FIG. 1. Backscattering coefficient density distributions
a: 1 — Nimbostratus (Ns-As), 2 — As
b: 1 — Dense Ns-As near frontal zone, 2 — St
c: Stratocumulus (Sc)
d: Optical depth density distribution N(τ) derived from the Kosmos-320 satellite images.

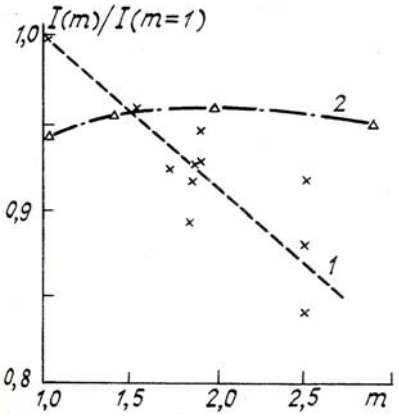

FIG. 2. Air-mass dependence of the radiation Intensity around 11.1 μm.
1 — outgoing intensity ratio $I_V(m)/I_V(m = 1)$ for high clouds with radiation temperatures of 200 — 220 K;
2 — angular distribution of $I_V(m)/B(T_C)$ at the cloud-base level obtained from airborne measurements.

Comparison of ε_v values obtained in this paper with similar measurements[12,13] shows general agreement as far as the mean values $\bar{\varepsilon}_v$ are concerned. It is interesting to analyze the altitude behavior of the integrated cloud emissivity $\hat{\varepsilon}_v$ obtained from hemispherical radiation fluxes. It follows from Ref. 14 that $\hat{\varepsilon}_v = \bar{\varepsilon}_v + \sigma_\varepsilon$, which is the sum of the mean emissivity and its r.m.s. deviation, and which characterizes the upper limit of the emissivity fluctuation for thick clouds in midlatitude regions, decreases from 0.96 + 0.30 to 0.82 + 0.76 with increasing cloud-top height from 1 to 6 — 7 km. One of the reasons for this is the cooling of the layer near the cloud top.

The cloud-top height was estimated through a comparison of the radiation height h_r calculated from measured self-radiation in the 10 — 12 μm range and the photometric height h_{ph} found separately from the measured reflected solar radiation in the oxygen absorption band at 0.76 μm. According to Ref. 15, the r.m.s. value of the height difference $\Delta h = h_r - h_{ph}$ is about 1.2 km.

This technique was also used for data processing of the Kosmos-1151 satellite images obtained from a spaceborne multichannel radiometer[8] and a photometer[16].

Figure 3 presents a regression curve for h_r and h_{ph} derived along a scan line of the satellite image over the tropical zone of the Indian Ocean on 18 July 1980. The test area was 2000 km long, with the air mass varying from 2.10 to 2.16. The r.m.s. deviation σ_ζ calculated using 345 data points was 0.09, which corresponded to σ_h = 1.16 km.

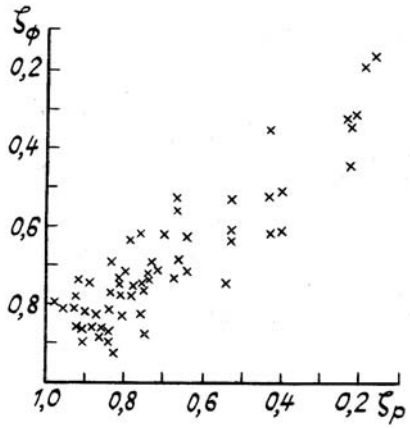

FIG. 3. Regression curve for h_r and h_{ph} extracted from the Kosmos-1151 satellite images at 11,1 and 0,74 — 0,76 μm, respectively.

In addition to geometrical factors associated with different fields of view of the instruments used, the discrepancy between the heights Ah is also caused by stochastic variations of the atmospheric physical parameters[17]. In the IR region these are the pressure and temperature at the cloud-tops and the profiles of temperature $T(\xi)$ and relative humidity $a(\xi)$ in the atmospheric layer over the clouds. The radiation height of clouds is determined from the relation

$$B_\nu [T(\zeta_r)] = I_\nu/\varepsilon_\nu V_\nu(\zeta_r) \quad (2)$$

$$T(\zeta_r) = B_\nu^{-1} \quad (3)$$

where $V_v(\zeta_r)$ is the transfer function of the overcloud layer, $\zeta = p(h_c)/p_0$ is the reduced pressure. The assumption that $\varepsilon_v = 1$ and $V_v = 1$ results in an over estimate of the cloud height, i. e., $\zeta_r < \zeta_c$, $h_r > h_c$. An inversion in $T_a(\zeta)$ introduces further errors in ζ_r given by Eq. (3). These errors Eire typical of very high clouds near the tropopause.

The photometric height h_{ph} is derived by assuming that the altitude distribution of oxygen is known and the ratio $S(\zeta_\phi)$ of the brightness values measured within the absorption band at 0.76 μm is determined by the transmission function $P_{\Delta v}[u(\zeta_{ph}), m]$, taking into account the spectral behavior of the extraterrestrial solar radiation $I_\odot(\lambda)$:

$$S(\zeta_{ph}) = \frac{I(0.76)}{I(0.74)} = P_{\Delta\nu}[u(\zeta_{ph}), m] \frac{I_\odot(0.76)}{I_\odot(0.74)}$$

$$P_{\Delta\nu}[u(\zeta_{ph}), m] = \exp(-m\zeta_{ph}^{2})^{\Delta\nu},$$

and is a single-valued function of ζ_{ph}. However, the ratio also depends on the photon paths within the cloud. For homogeneous clouds, neglect of the

increased photon path lengths would lead to an underestimate of the height, i.e. $\zeta_{ph} > \zeta_c$, ($h_{ph} < h_c$). In the case of inhomogeneous clouds with a semitransparent upper layer there is a "multipass-cell" effect, which, in turn results in a "negative" height ($h_{ph} < 0$). Thus, a comparison of h_r and h_{ph} yields $h_{ph} < h_c < h_r$. If the measurements give $h_{ph} < 0$ and $h_r > 0$ then the foregoing considerations lead us to suggest a multilayer cloud structure. A serious uncertainty in h_{ph} is introduced by the "saturation" of the transmission function for oxygen $P_{\Delta v}[u(\zeta_{ph}), m]$ within the lower clouds due to multiple scattering and blurring of the oxygen absorption band. For large air masses $m = \sec\theta_\odot + \sec\theta$, where $\theta_\odot$ and θ are the solar and $I\Delta v$-measurement zenith angles, respectively.

These peculiarities in the behavior of $P_{\Delta v}[u(\zeta_{ph})]$ are illustrated by the measurement results presented in Fig. 4, which shows a segment of the spatial cross-section of the radiation temperature T_r at 11.1 ± 0.18 μm, the cloud brightness at 0.74 μm and the brightness ratio $S(\zeta_{ph})$.

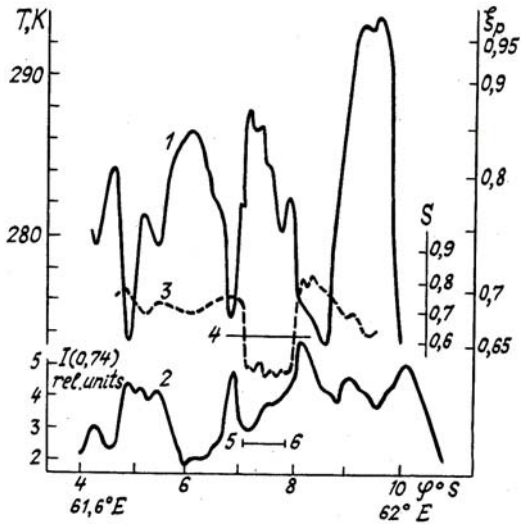

FIG. 4. Radiative properties of clouds retrieved from theKosmos-1151 satellite images over the Indian Ocean on 18 July, 1980.
(1) Radiation temperature T_r and cloud top height (ζ_r).
(2) Brightness of reflected solar radiation I(0.74).
(3) Intensity ratio S = I(0.76)/I(0.74) in the oxygen absorption band and in the atmospheric window.
(4) Intensity ratio from Curve 3 for clear-sky conditions.
(5), (6) Boundaries of multilayer cloud area.

As seen from Fig. 4, setting the transmission function $P_{\Delta v} = 0{,}63$ for clear-sky conditions detected by IR enables one to detect a multilayer structure with $h_{ph} < 0$ and $0.51 \le P_{\Delta v} \le 0{,}55$. The multilayer quality of the cloud system accompanied by a semitransparent upper layer will also tend to enhance the IR radiation attenuation. The resulting decrease of intensity $I_{\Delta v}$ and radiation temperature T_r may be determined from the angular distribution $I_{\Delta v}(m)$. Figure 5 presents the spectral distribution function $I_{\Delta v}(m)$ in the 10–18 μm range for the air masses $m_1 = 1$ and $m_2 = 2.6$ corresponding to endpoints of line 5–6 with $h_{ph} < 0$. A comparison of radiation temperatures and their differences ΔT_r for $\lambda = 11{,}1$ μm,

$$\Delta T_r(v, m_1, m_2) = T_r(v, m_1 = 1{,}0) - T_r(v, m_2 = 1{,}6),$$

suggests that ΔT_r at points 5 and 6 increases from 8 to 13 K. The fact that $S(\zeta_{ph})$ is approximately constant within the interval 5–6, and as a consequence, h_{ph} is invariant as well, suggests that ΔT_r is further decreased by 5 K at point 6 in the upper cloud layer. This example demonstrates the feasibility of identification of a double-layer cloud system such as, for example, a combination of Ci and middle or lower clouds.

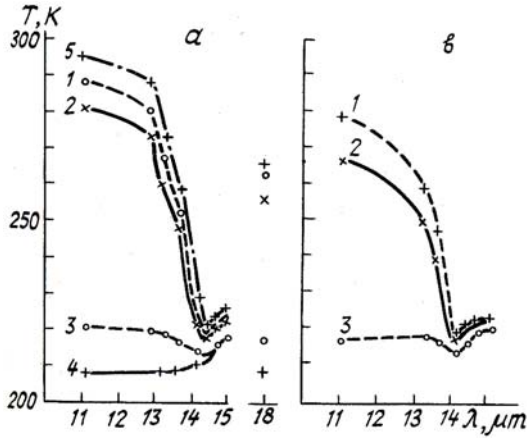

FIG. 5. Spectral distribution of radiation temperature $T_r(v)$ as measured on 18 July 1980 over the Indian Ocean, (a) Air mass $m_1 = 1$. (1) and (2) Spectra of a portion of the cloud at points 5, 6 from Fig. 4, respectively; (3) and (4) High cloud spectra; (5) Clear sky region; b is for air mass 1.6. (1)–(3) the same as in curves 1–3 (a).

Measurements of the I_v spectral behaviour contribute to improved accuracy in cloud-top height estimates. The computational procedure for ζ_r is merely to search for a minimum of the functional

$$F = \sum_i \frac{\Delta^2}{\sigma_i^2} [\tilde{I}_i(\zeta_r) - \tilde{I}_i]^2$$

where $\tilde{I}_i(\zeta_r)$ and $\tilde{I}_i$ are the calculated and measured deviations of the radiation intensity, $i = 1, \ldots, N$ is the number of the spectral channel, $\tilde{I}_i = I_{vi} - I_{vi}(\zeta_c)$, is the measured intensity, $I_{vi}(\zeta_c)$ is the calculated intensity for a cloud at height ζ_c.

Concurrent measurements of the radiation temperature T_r in the IR and of the brightness temperature T_b inthe microwave region[8] enable one to

ascertain the dominant phase fraction of the cloud. The technique for distinguishing between water droplets and mixed clouds is based on the fact that measurements at wavelengths from region 0.4 cm to 0.8 cm provide for identification of water droplet clouds and estimation of their liquid water content, whereas the identification of ice crystal clouds in this spectral region is too difficult, as absorption by ice crystals is about two orders of magnitude weaker than that of liquid water droplets. In addition, the IR measurements in the 10–12 μm atmospheric window make it possible to estimate the cloud-top temperature and calculate the increment of radiation temperature ΔT_r,

$$\Delta T_r = T_s - T(\zeta_r),$$

where T_s and $T(\zeta_r)$ are the retrieved temperatures of the earth's surface and clouds, respectively.

The measurement data obtained from the Kosmos-243 and Kosmos-320 satellite images have revealed correlations between the temperature increment ΔT_r, the integrated water content w*, and the phase state (see Table 3).

Table 3. Properties of cloud phase structure

Temperature contrast ΔT_r K	Integrated water content w kg/m^2	Correlation coefficient $r(T_r, T_b)$	Phase state
< 25	0.05	-0.2+ 0.0	water-droplets
> 25	0.03	0.0	mostly ice crystals
10 - 30	0.05-0.2	-0.8+-0.6	mostly water-droplets
		0.0	
15 - 60	0.20-0.6	-0.8+-0.6	mostly water-droplets
		0.0	considerable amount of ice, mixed clouds

The analysis of the cloud system parameters taking synoptic information on cloud forms into account has shown that the correlation coefficient $r(T_r, T_b)$ for temperatures measured in the IR and microwave regions is nearly zero in all the cases where cirrus clouds occur at $\Delta T_r > 25$ K. At high correlation coefficients ($r = -0.6$ to -0.8), the water droplet phase is found to prevail. It should be noted that the IR and microwave measurements are independent of the observation time, while the feasibility of photometric measurements on reflected solar radiation[5] is strongly contingent upon lighting conditions.

REFERENCES

1. K.Ya. Kondratjev and Yu.M. Timofeev *Meteorological Sensing of the Atmosphere from Space* (Gidrometizdat, Leningrad, 1978)
2. W.L. Smith and C.M.R Platt *Comparison of satellite-deduced Cloud Heights with Indications from Radiosonde and ground-basedlaser measurements* J. Appl. Meteorol., No. 17, 1799 (1978)
3. A.K. Gorodetskii, M.C. Malkevich and V.I. Syachinov *Determination of Cloud Heights from Kosmos-320 Satellite* Doklady Akad. Nauk SSSR, 200, No. 3, 588
4. V.A. Golovko *Investigation of the Accuracy of Cloud Identification in the Viewing Band of Satellite IR Spectrometer* Proc. Gos. NIITsIPR, No. 15, 4 (1982)
5. M.S. Malkevich, V.V. Badaev, V.S. Malkova, et. al. *Methods and Results of the Determination of Cloud Properties from Satellites* Proc. 9th International Cloud Physics Conf. (Tallinn "Valgus", 1984)
6. A.K.Gorodetskii, D.T.Matveev, E.P.Dombkovskaya et.al. Determination of the Phase State of Clouds from Satellites Meteorologiya i Gidrologiya, 66 (1975)
7. A.K. Gorodetskii, A.P. Orlov, E.M. Kozlov, et. al. Izvestiya Akad. Nauk SSSR, ser. Fizika Atmosfery i Okeana, **13**, 424 (1977)
8. A.K. Gorodetskii, B.G. Kutuza, M.S. Malkevich lssled. Zemli iz Kosmosa, 3 (1986)
9. A.K. Gorodetskii, I.S. Kuznetsov, V.E. Lystsev, et. al. Izvestiya Akad. Nauk. SSSR, ser. Fizika Atmosfery i Okeana, **16**, 705 (1980)
10. G.V. Rozenberg, M.S. Malkevich, V.S. Malkova, et. al. Izvestiya Akad. Nauk SSSR, ser. Fizika Atmosfery i Okeana, **10**, .14 (1974)
11. G.V. Rozenberg, G.K. Iljich, S.A. Makarevich, et. al. Izvestiya Akad. Nauk SSSR, ser. Fizika Atmosfery i Okeana, **6**, (1970).
12. G.L. Stephens, G.W. Paltridge, and C.M.R. Platt Radiation properties in extended water clouds Observations J. Atmos. Sci., 1978, **35**, 2133
13. I.S. Reshetnikova and O.I. Popov Izvestiya Akad. Nauk SSSR, ser. Fizika Atmosfery i Okeana, **6**, 639 (1970)
14. S.K. Cox J. Atm. Sci., **33**, No. 2 (1976)
15. M.S.Malkevich *Optical Studies of the Atmosphere from Spaceborne Platt forms* (Nauka, Moscow, 1973)

16. G.A. Tolkachenko and R.R. Stanichnaya *The Factor Structure of Brightness of the Atmosphere Ocean System* in: *Remote. Sensing of the Ocean.* (MGI Akad. Nauk Ukrainskoi SSR, Sevastopol, 1982)
17. Yu.M. Timofeev Problemy Fizik.i Atmosfery, No. 16, **80** (1986)